电 化 学
J. Electrochem. 2022, 28(11), 2219007 (1 of 18)

[Review] DOI: 10.13208/j.electrochem.2219007 http://electrochem.xmu.edu.cn

Advances and Atomistic Insights of Electrolytes for Lithium-Ion Batteries and Beyond

Tingzheng Hou[1,2*], Xiang Chen[4], Lu Jiang[1], Cheng Tang[3,4*]

(*1. Department of Materials Science and Engineering, University of California, Berkeley, CA 94720, USA; 2. Institute of Materials Research, Tsinghua Shenzhen International Graduate School, Tsinghua University, Shenzhen 518055, China; 3. School of Chemical Engineering and Advanced Materials, The University of Adelaide, Adelaide, SA 5005, Australia; 4. Beijing Key Laboratory of Green Chemical Reaction Engineering and Technology, Department of Chemical Engineering, Tsinghua University, Beijing 100084, China*)

Abstract: Electrolytes and the associated electrode-electrolyte interfaces are crucial for the development and application of high-capacity energy storage systems. Specifically, a variety of electrolyte properties, ranging from mechanical (compressibility, viscosity), thermal (heat conductivity and capacity), to chemical (solubility, activity, reactivity), transport, and electrochemical (interfacial and interphasial), are correlated to the performance of the resultant full energy storage device. In order to facilitate the operation of novel electrode materials, extensive experimental efforts have been devoted to improving these electrolyte properties by tuning the physical design and/or chemical composition. Meanwhile, the recent development of theoretical modeling methods is providing atomistic understandings of the electrolyte's role in regulating the ion transport and enabling a functional interface. In this regard, we stand at a new frontier to take advantage of the revealed mechanistic insights into rationally design novel electrolyte systems. In this review, we first summarize the composition, solvation structure, and transport properties of conventional electrolytes as well as the formation mechanism of the electrode-electrolyte interphase. Moreover, some of the promising energy storage systems are briefly introduced. Further, approaches to stabilize the electrode-electrolyte interphase using novel electrolyte design, including electrolyte additives, high-concentration electrolytes, and solid-state electrolytes, are discussed. Some recent advances in the atomistic modeling of these aspects are particularly focused to provide a fundamental understanding of electrolytes and a comprehensive guide for future electrolyte design. Finally, we highlight the prospects of theoretical screening of novel electrolytes.

Key words: lithium-ion batteries; electrolytes; atomistic modeling; solid electrolyte interphase; solid-state electrolytes

1 Electrolytes: Key to Next-Generation Energy Storage

High-capacity energy storage technology holds a decisive position in fulfilling the ever-increasing demands of portable electronic devices, electric vehicles, and smart grids for intermittent solar or wind power[1, 2]. Conventional lithium-ion batteries (LIBs) with a composition of $LiCoO_2$/graphite, which has a theoretical energy density of 360 $Wh \cdot kg^{-1}$, cannot fully satisfy this requirement. To further increase the energy density, novel cathode materials (e.g., cation-disordered rocksalt-type cathode materials[3, 4], sulfur/carbon composite cathode[5]) and anode materials (e.g., silicon anode[6], Li metal anode[7]) emerge as promising candidates for realizing next-generation energy storage. Along with the innovation of electrode mate-

Cite as: Hou T Z, Chen X, Jiang L, Tang C. Advances and atomistic insights of electrolytes for lithium-ion batteries and beyond. *J. Electrochem.*, 2022, 28(11): 2219007.

Received: 2022-09-11, Revised: 2022-10-10. *Corresponding author, Tingzheng Hou: +1-5109938393; Cheng Tang: 86-10-62789041, E-mail: tingzheng_hou@berkeley.edu (T. Hou), cheng.tang@adelaide.edu.au (C. Tang)

rials, electrolytes that enable Li^+ transport between electrodes during charging and discharging require to be redesigned as well. This is particularly important because the as-formed electrode-electrolyte interphase is found to be crucial for reversible cell operation. Therefore, the actual performance of an electrode material is largely dependent on the composition and intrinsic properties of the associated electrolyte.

2 Understanding Conventional Electrolytes of LIBs

2.1 Electrolyte Components and Solid Electrolyte Interphase

After decades of intensive development, the skeletal composition of the electrolyte for commercialized LIBs has long been established[8]. Although differing among manufacturers and scenarios, the majority of electrolytes employ the carbonate electrolyte formula with cyclic carbonates (e.g., ethylene carbonate (EC), and propylene carbonate (PC)), linear carbonates (e.g., ethyl methyl carbonate (EMC), diethyl carbonate (DEC), and dimethyl carbonate (DMC)) and lithium salts (e.g., $LiBF_4$, $LiPF_6$, and lithium bis(trifluoromethanesulfonyl)imide (LiTFSI)), as shown in Tables 1 and 2. The high dielectric constant of cyclic carbonates presents the ability to dissolve the lithium salt; the linear carbonates are utilized as co-solvents to mitigate the viscosity and lower the melting point of the electrolyte; the lithium salt is required to be dissociated in the electrolyte to some extent which enables the free Li^+ transport, and should be electrochemically stable toward both electrodes. Moreover, the electrically insulating and ionically conductive solid electrolyte interphase (SEI) between anode and electrolyte is spontaneously formed by the reduction reactions of electrolytes in the initial cycles[9].

An optimal SEI layer passivates the anode surface against further side reactions while facilitating Li^+ transport[10-12]. When the electrolyte reductive stability limit is reached during the initial charging of a Li-ion

Table 1 Common carbonate solvents in LIB electrolytes.

Cyclic carbonate		Linear carbonate		
EC	PC	DMC	DEC	EMC
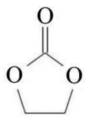	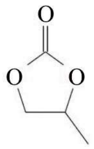	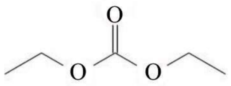	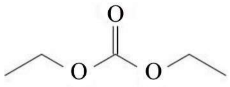	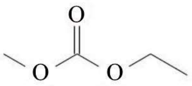
High dielectric constant		Low viscosity Lowmelting point		

Table 2 Common salts in LIB electrolytes.

$LiBF_4$	$LiPF_6$	LiTFSI
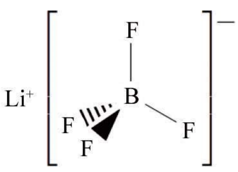	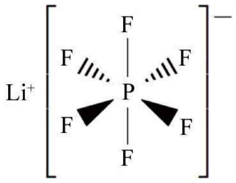	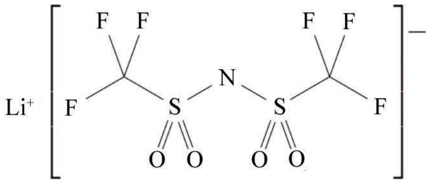
Electrochemical stability Ability to dissolve and dissociate		

battery, a cascade of interdependent reactions—including reduction, oxidation, bond cleavage, and bond formation—spontaneously occur to form an SEI on the battery anode surface[13]. The initially formed SEI containing inorganic species, e.g., LiF, Li_2CO_3, and $Li_2C_2O_4$[14, 15], as well as organic ones, e.g., lithium ethylene dicarbonates (LEDC) and lithium ethylene monocarbonate (LEMC)[16-18], further evolves through a variety of aging processes[19-22] (hydrolysis, reaction between Li salt and intermediate decomposition products, and thermal decomposition, etc.) as well as continuous electrolyte reduction[23, 24]. It has also been observed that gases (particularly H_2, C_2H_4, and CO) are produced as byproducts of SEI formation[25]. The sequence of reactions and their aging depend both on the specific components and concentration, including additives and impurities, of the bulk electrolyte, and on the specific anode material and its surface chemistry and structure[12]. Hence, in principle, every anode material requires a differently tailored electrolyte, to achieve maximal compatibility—both electrochemically as well as mechanically.

2.2 Solvation Structure

The first step to understand the mechanisms of SEI formation is to understand the solvation chemistry of electrolyte species. When electrolytes react with the anode surface to form the SEI, the reaction products are highly dependent on the starting reactants as well as their immediate solvation environment[26]. There has been a long-existing confusion and controversy on the detailed solvation structure of carbonate-based electrolytes, in particular the ones of commercial interest. Instrumental measurements including infrared spectroscopy (IR)[27-29] and Raman[30, 31] have been utilized to determine the ion-solvent coordinating states. However, challenges remain for quantitatively interpreting the spectroscopic fingerprints of multi-component electrolytes. It is difficult to quantitatively deconvolute the overlapping peaks of different carbonate species, the overtone peaks, and the accompanied Fermi resonance effects, especially when solvents share the same functional groups[32]. In addition, because of the possible difference in spectroscopic sensitivity between the coordinated and uncoordinated states of solvent moieties, the scaling of peak area integrals is required to obtain the actual molar ratio of species, which could introduce additional error and hinders straightforward quantitative interpretation. Most recently, the internally referenced diffusion-ordered spectroscopy (IR-DOSY)[32, 33] has been utilized to construct a solvating power series, which provides a reliable quantitative measure of the lithium solvating power of common electrolyte solvents. Using the as-established solvating power series, researchers can easily evaluate the solvation state of an individual solvent in a binary or ternary electrolyte system. This reported solvating power series will provide insightful guidance for the future design of functional electrolyte system and will be especially instructive in the selection of suitable solvent/co-solvent for lithium batteries.

As an alternative approach, computational methods including *ab initio* molecular dynamics (AIMD)[34-36] and classical molecular dynamics (MD)[37-41] simulations have shown satisfying results in modeling the solvation and transport behaviors. For example, Hou et al. [26] revealed the different roles of the Li salt, cyclic carbonate, and linear carbonate in tailoring the solvation structure, ionic conduction, and reduction reactions of mixed-carbonate electrolytes (MCEs, Figure 1a), the one of broad commercial interest. The EC-base (1.2 $mol\cdot L^{-1}$ $LiPF_6$ in EC) and Gen2 (1.2 $mol\cdot L^{-1}$ $LiPF_6$ in EC and EMC) electrolytes were investigated using MD simulations, quantum chemical calculations, and experimental measurements. While the $LiPF_6$ salt in the EC-base electrolyte was mostly dissociated (Figure 1b), the Gen2 electrolyte exhibited a much higher degree of ion correlation and association (Figure 1c). Interestingly, and non-intuitively, in the Gen2 electrolyte, the coordination number of EC with Li^+ decreased when PF_6^- entered the first solvation shell. The electrostatic repulsion between the highly polarizable EC and the negatively charged anion PF_6^- was identified as responsible for the phenomenon. Importantly, the anion-solvent exchange in MCEs was for the first time reported to be predomi-

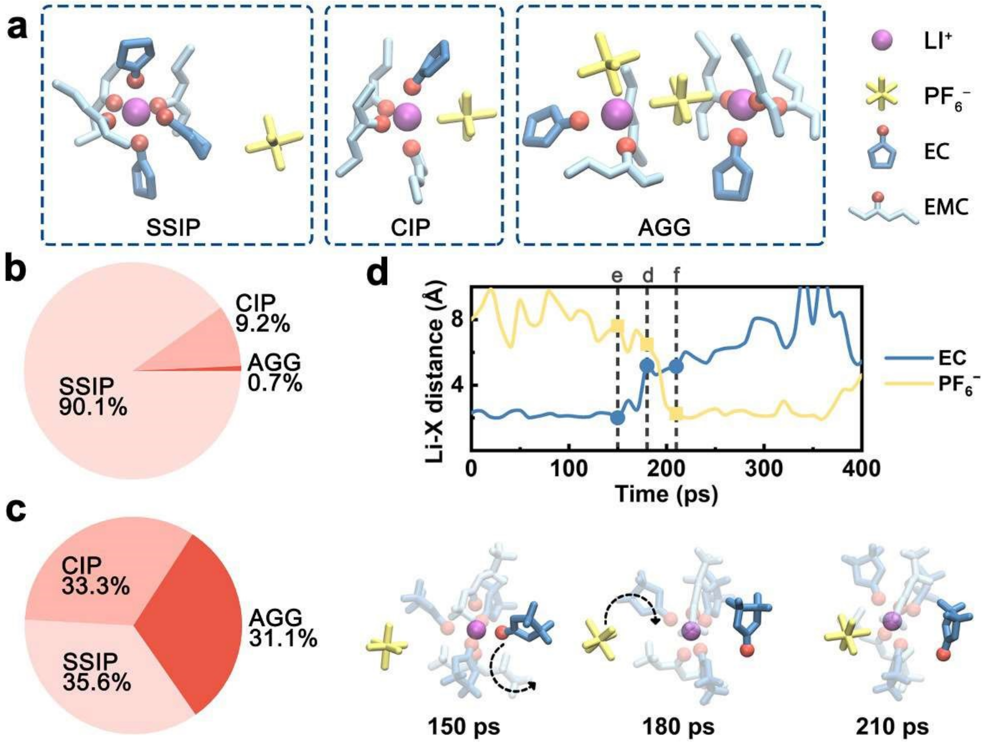

Figure 1 (a) Three representative solvation structures of solvation separated ion pairs (SSIP), contact ion pairs (CIP), and aggregate (AGG) species in the Gen2 electrolyte. The population of SSIP, CIP, and AGG species in (b) EC-base and (c) Gen2 electrolytes. (d) Sample trajectory of EC-PF_6^- exchange in the Gen2 electrolyte. Reproduced with permission from ref [26]. Copyright 2019 The Authors. (color on line)

nantly "exit-entry" type with identified energetic and electrostatic origins (Figure 1d). This mechanism explains the non-intuitive preferential removal of cyclic carbonates (such as EC) from the Li^+ solvation shell upon the forming of a contact-ion pair, a phenomenon which has long baffled the LIB electrolyte community.

2.3 Ion Transport and Interphasial Chemistry

These insights on electrolyte solvation structures have strong implications for the transport behavior of practical LIB electrolytes with mixed ingredients as well as the SEI formation process. In terms of the ionic conduction of MCEs, for example, the Nernst-Einstein equation is not applicable for calculating the ionic conduction from self-diffusion coefficients in such complex systems due to significantly correlated ion motions[42, 43]. Most recently, Fong et al.[26, 44-48] utilized the Onsager Transport framework as a rigorous methodology to analyze transport properties in electrolytes (Figure 2a). The application of the theoretical framework provides a new and accurate tool for describing the ion transport that can successfully capture the ion correlations in MCEs. As shown in Figure 2b, in contrast to the EC-base electrolyte, the Gen2 electrolyte exhibited greater self-diffusion coefficients due to the lower viscosity of the linear carbonates[26]. Therefore, although the Gen2 electrolyte exhibited more aggregates and bulky conductive species, the overall ionic conductivities of the Gen2 and EC-base electrolytes were very similar (Figure 2c).

Further, with the revealed solvation structures and transport properties, mechanistic-level stochastic simulations are made possible to model the SEI formation and evolution reactions. For example, Spotte-Smith et al. [49] used one-dimensional kinetic Monte Carlo (kMC) simulations based on reaction mechanisms obtained via automated computational reaction networks analysis and *ab initio* calculations to

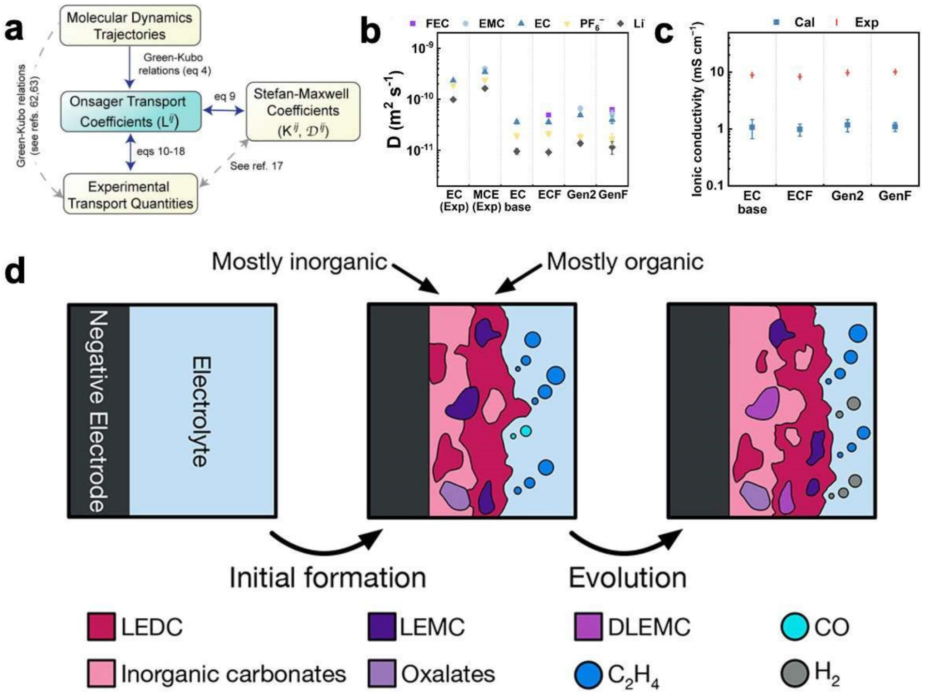

Figure 2 (a) Outline of the relationships between the Onsager transport coefficients and other aspects of transport. Reproduced with permission from ref [48]. Copyright 2021 The Authors. (b) The calculated self-diffusion coefficients of electrolyte species (EC, EMC, FEC, PF_6^-, and Li^+) in the EC-base, ECF, Gen2, and GenF electrolytes. (c) The experimental (Exp) and calculated (Cal) ionic conductivity at 298 K. Reproduced with permission from ref [26]. Copyright 2019 The Authors. (d) Mechanistic model of the SEI formation. Reproduced with permission from ref [49]. Copyright 2022 The Authors. (color on line)

study SEI formation and evolution of a practical electrolyte system. Without any fitting parameters to experimental inputs, the theoretical model only utilized the simulated solvation structures and transport properties as well as the calculated free energy of reaction fragments. By conducting simulations over a range of applied potentials and with varying electron tunneling barriers, the formation of distinct inorganic (e.g., LEDC, LEMC) and organic (e.g., inorganic carbonates) layers in the SEI were observed, as shown in Figure 2d. Competition between organic and inorganic SEI products was found to be driven primarily by the different reduction mechanisms of Li^+-EC, as well as the direct reduction of CO_2. By performing simulations at elevated temperatures, the expected electrochemical decomposition of LEDC was observed to form inorganic carbonates. The above efforts demonstrate the promise of data-driven simulations from bulk electrolyte properties toward explaining the most-concerned SEI formation process.

3 Novel Electrochemistry in Li-Ion Batteries and Associated Challenges for Electrolyte Design

3.1 Anodes

There is intense interest in developing new anode materials that store higher densities of lithium[50]. One of the most promising anode materials for future high energy density LIBs is Si, due to its high theoretical specific capacity (exceeding 4200 mAh·g^{-1}) and low cost[6]. However, as shown in Figure 3a, during the charging and discharging process, the Si anode must suffer a large volume change during battery reactions, i.e., up to 280% volume expansion (increase) from Si to $Li_{15}Si_4$, compared with 13.2% volume expansion from C_6 to LiC_6[51]. The non-passivating Si SEI formed in conventional LIB electrolytes is unable to mitigate the cracking due to Si's large volume expansion and contraction during cycling[8, 52]. To improve the Si SEI performance, there is a pressing need for functional,

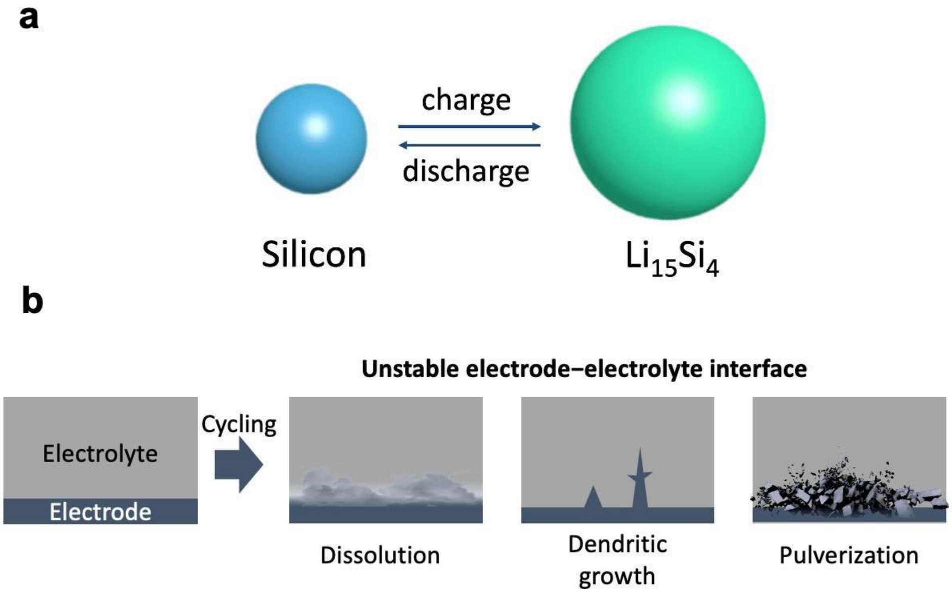

Figure 3 (a) Illustration of the volume expansion during the charging and discharging process of Si anodes. (b) Illustration of the unstable electrode-electrolyte interface during cycling. (color on line)

optimized electrolyte s with excellent bulk stability and conductivity while exhibiting a suitable range of passivating reactions toward the Si anode material[53, 54], for example, by utilizing modified salts and electrolyte additives[55, 56].

Beyond the Li-Si conversion chemistries, lithium metal is regarded as another promising anode to further increase the energy density of batteries because of its high theoretical specific capacity (3860 mAh·g^{-1}) and low reduction potential (−3.04 V vs. standard hydrogen electrode)[7]. However, uncontrollable lithium deposition during plating/stripping, generally emerging as dendritic and mossy lithium, induces cell failure and even thermal runaway causing fire/explosion events, which plague the utility of lithium metal anodes in practical applications[57]. Li dendrites are generally induced by inhomogeneous distributions of space charge, current density on the anode surface, and the crack of SEI. Much effort has been devoted to preventing the Li dendrite growth in a working battery[58]. Among these strategies, *in situ* formation of SEI with high uniformity and stability is one of the most effective and convenient routes due to its prominent impact and low cost, particularly in the industrial manufacture of batteries[52]. Many electrolyte modification approaches are employed to facilitate the *in situ* formation of a stable SEI layer, such as metal cation additives (Cs^+ and Rb^+)[59], fluoroethylene carbonate (FEC) additive[60], and high-concentration electrolyte[61].

3.2 Cathodes

Less consideration of the electrolyte design has been given to the cathode materials along with the cathode-electrolyte interphase (CEI) for conventional LIBs. However, the application of high-voltage cathode materials such as Ni-rich cathode materials[62] and cation-disordered rocksalt-type cathode materials [3] has raised new challenges for designing electrolytes with an expanded electrochemical stability window up to 5 V. Therefore, the design of electrolytes that are compatible with both novel lithium metal anode and high-voltage cathodes is very critical for high-energyrechargeable batteries. Beyond intercalation chemistry, the lithium-sulfur (Li-S) cathode is considered a breakthrough compared with layered oxide cathodes. Remarkable advantages include abundant resources, low costs, and high biocompatibility of cathode materials sulfur, as well as a high theoretical specific energy up to 2600 Wh·kg^{-1}[63]. However, one of the major problems in Li-S batteries is the so-called “shuttle” effect, which manifests as spontaneous dissolution and diffusion of soluble intermediates, polysulfides (PS), and a series of concurrent side reactions at interfaces or in solution[64]. The shuttle effect not only gives rise to a severe loss of active materials from the cathode, but also renders poor Coulombic efficiency and cycling life. Rational selection or design of optimal electrolytes with reduced PS solubility is critical in controlling the deleterious shuttle reactions and protecting the electrode surface[65]. In fact, Li salts used in traditional LIBs (e.g., $LiPF_6$, $LiBF_4$) and solvents (e.g., ester, carbonates, phosphates) are unsuitable for Li-S battery applications due to their parasitic reactions with PSs[65]. Therefore, so far, an ethereal electrolyte system with 1 $mol \cdot L^{-1}$ LiTFSI in a binary solvent mixture of 1,3-dioxolane and 1,2-dimethoxyethane (DOL/DME) is considered default for Li-S cells. However, although ethers are non-reactive with polysulfides, they dissolve polysulfides at high-concentration and hence encourage parasitic shuttling[66].

In summary, issues including but not limited to intermediate dissolution, dendritic lithium deposition, and pulverization are found to be detrimental for the capacity and cycling performance of novel cathode and/or anode materials, as shown in Figure 3b. Strategies including high-concentration electrolytes and localized high-concentration electrolytes have been considered as viable approaches to mitigate the issues. A more detailed discussion on these novel electrolyte designs will be presented in the following sections.

4 Novel Electrolyte Design

4.1 Electrolyte Additive

For both Si and Li metal anodes, FEC has been spotlighted as an effective electrolyte additive that significantly enhances the stability and elasticity of the as-formed SEI film[60, 67]. As shown in Figure 4a, in the presence of FEC, which degrades at a higher reduction potential than that of both EC and DEC, a denser, more uniform, and conformal SEI is formed on both silicon anode and lithium metal anode[60, 68]. This SEI layer has been found to ameliorate the emergence of large cracks and suppress further decomposition of EC/DMC, leading to enhanced electrochemical performance, improved Coulombic efficiency, and uniform surface morphology of the anode (Figure 4b). To understand the composition and morphology of the Si SEI formed with FEC, extensive experiments using scanning transmission electron microscopy (STEM)[69], electron energy loss spectroscopy (EELS)[69], Fourier-transform infrared spectroscopy (FTIR)[55, 70], X-ray photoelectron spectroscopy (XPS)[6, 71], atomic force microscopy (AFM)[72, 73], hard X-ray photoelectron spectroscopy (HAXPES)[68, 74], nuclear magnetic resonance (NMR)[6, 75], differential electrochemical mass spectrometry (DEMS)[76], and time-of-flight secondary ion mass spectrometry (TOF-SIMS)[77], etc., have been undertaken. Lucht and co-workers[55] suggested that a 10% content of FEC can provide the optimal improvement on the base carbonate electrolyte in terms of impedance and capacity retention. Subsequent studies found that, compared with a standard EC/DMC electrolyte, the use of 10% FEC additive modified the organic SEI components derived from LEDC and soluble linear oligomers to soluble and insoluble crosslinked poly (ethylene oxide)-based polymers (such as lithium poly (vinylene carbonate)), which could better passivate the anode surface and resist volume expansion[6, 75, 78]. Meanwhile, FEC incurs increased formation of LiF, and less formation of Li_2CO_3 and organic carbonate species, resulting in an overall lower interfacial impedance of the Si anode[79]. Moreover, there is evidence that FEC influences the $LiPF_6$ decomposition reaction and may suppress further salt degradation after the initial cycles[68]. Hou et al.[12] investigated the influence of FEC on $LiPF_6$/EC electrolytes for Si anodes through classical MD, FTIR, and quantum chemical calculations. Albeit a minority species, FEC was found to significantly modify the solvation structure and reduction behavior of the electrolyte while being innocuous to transport properties. Even with limited 10% FEC, the Li^+ solvation structure exhibited a notably higher contact-ion pair ratio (14%) than that of parent EC electrolyte (6%). Moreover, FEC itself, as a new fluorine-containing species, appeared in 1/5 of the Li^+ solvation shells. As shown in Figure

4c, the Li^+-coordinated FEC was found to reduce prior to EC and uncoordinated FEC, thus passivating the anode surface at an early onset (ca. 0.3 V higher than EC) by forming LiF and polymeric species. The critical role of FEC in tailoring the Li^+ solvation structure and as-formed protective SEI composition provides mechanistic insight that will aid in the rational design of novel electrolyte additives.

A follow-up study provides another excellent example for designing electrolyte additives by regulating the solvation chemistry and reduction reactions[80]. A series of additive for the $LiPF_6$/PC electrolyte were investigated in a Li metal battery, including EC, VC (vinylene carbonate), FEC, and VEC (vinyl ethylene carbonate). MD simulations showed that all additives can enter the first solvation sheath of Li^+. The solvating ability of the additives follows the order of VEC >EC ≈ FEC ≈ VC, which indicates that VEC has the strongest solvating ability. With higher reduction potentials of FEC and VEC over PC, they are preferentially reduced on the anode surface during the early state of the battery to form a protective SEI, and the reduction of the solvent (PC) or salt ($LiPF_6$) is suppressed. However, for EC and VC, even though they have a similar solvating ability to FEC, they cannot form stable SEI on the lithium metal anode because of a lower reduction potential and unstable reduction products.

4.2 High-Concentration Electrolytes

Several promising liquid electrolytes including high-concentration electrolytes (HCE) and localized high-concentration electrolytes (LHCE) have been

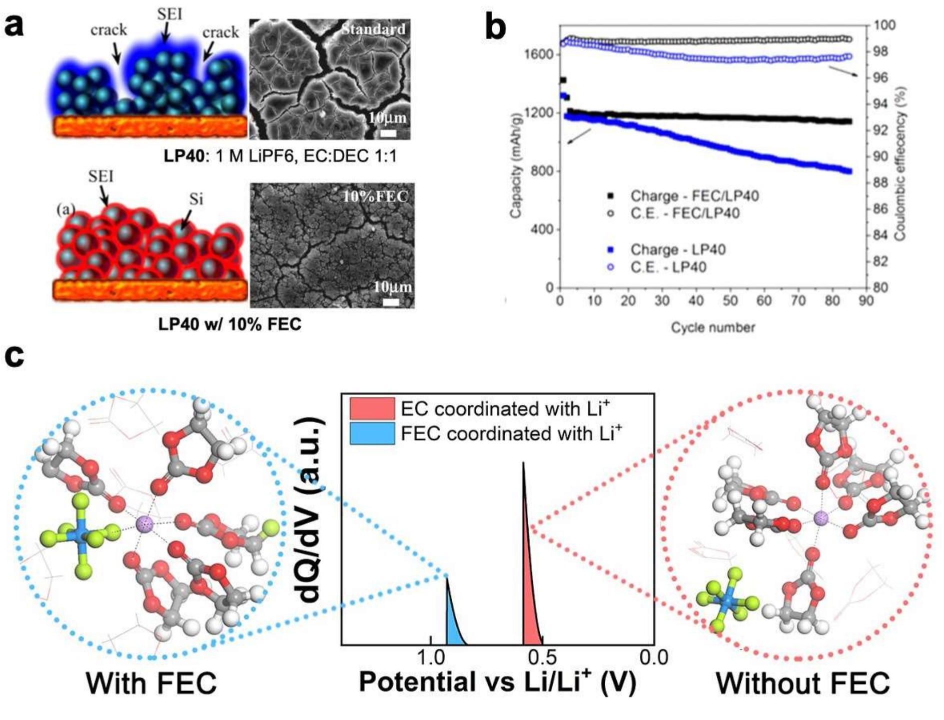

Figure 4 (a) Schematic representation and scanning electron microscopic images of SEI formation on a silicon anode which is long-time cycled with different electrolytes LP40 (1 mol·L^{-1} $LiPF_6$ in EC/DEC 1:1 wt.) and FEC LP40 (90wt% LP40 and 10wt% FEC). The two SEI layers are different in composition and are highlighted with different colors. (b) Gravimetric capacities and Coulombic efficiencies of the Si/Li half-cells cycled between 0.12 and 0.9 V at 500 mA·g^{-1} (Si) using FEC/LP40 (black) and LP40 (blue) electrolytes. (c) Schematic representation of the preferential reduction of Li^+-coordinated FEC over EC and uncoordinated FEC, which provides earlier onset SEI formation and anode passivation. The schematic representation and cycling performance reproduced with permission from ref [68]. Copyright 2015 American Chemical Society. The SEM images are reproduced from ref [55]. Copyright 2014 The Electrochemical Society. The schematic representation is reproduced from ref [12]. Copyright 2019 The Authors. (color on line)

designed to tune the SEI chemistry as well as increase the oxidation stability of the electrolyte at the cathode side. Specifically, HCE has been reported to provide increased oxidative stability, absence of exfoliation, low volatility, higher charge density, and preferred ion transport[81, 82]. In HCE, significant ion-pairing and aggregation occur, while limited solvent molecules therein are largely bound to cations, leading to entirely new structures at both molecular and long-range scales. The reduction products of HCE that form the SEI bear inorganic-rich chemical signatures derived from the anions instead of the solvent molecules, such as LiF. While these competitional changes can be clearly characterized, rare solvation structure and transport properties have been observed in HCE which are not yet fully understood. For example, as shown in Figure 5a, in aqueous "water-in-salt" electrolyte (WiSE) by Suo et al.[83] based on LiTFSI dissolved in water, a significant "disproportionation" in Li^+-solvation sheath was observed in both MD simulation (Figure 5b) and experiments (Figure 5c), leaving a high portion (40%) of Li^+ exclusively surrounded by water molecules only, while the rest are mainly surrounded by TFSI, which in longer length leads to a heterogeneity on nano-scale (1 nm) with water-rich and anion-rich regions[84]. One benefit of the liquid structure with nano-heterogeneity is the fast Li^+ transport, which is enabled by the high fraction of free Li^+ via vehicular motions through the water-rich region. It should be noted that the question remains unanswered regarding the specific mechanisms governing the formation of such structures.

The potential advantages of HCE are not without drawbacks. The high salt concentration not only induces compromises in conductivity and viscosity, but also drives up the cost of the electrolyte[85]. In comparison to HCE, LHCE can mitigate these problems owing to the introduction of inert diluents (non-coor-

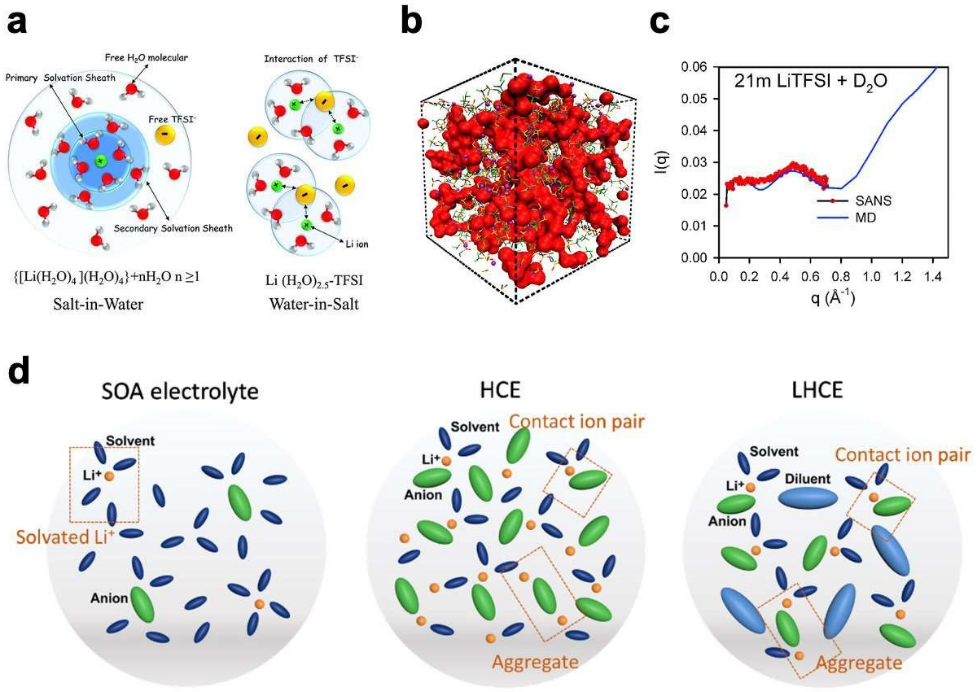

Figure 5 (a) Illustration of the evolution of the Li^+ primary solvation sheath in diluted and water-in-salt solutions. Reproduced with permission from ref [83]. Copyright 2015 American Association for the Advancement of Science. (b) 3D snapshot showing an interconnected H_2O domain in red and TFSI anions as wireframe from MD simulations of 21 m LiTFSI-H_2O at 298 K. (c) Structure factor from small-angle neutron scattering (SANS) experiments and MD simulations for 21 m (molality) LiTFSI in D_2O. Reproduced with permission from ref [84]. Copyright 2017 American Chemical Society. (d) Comparison of the solvation structures of conventional electrolyte, HCE, and LHCE. Reprinted with permission from ref [86]. Copyright 2021 The Authors. (color on line)

dinating co-solvent)[86]. Polyfluorinated ethers, such as bis(2,2,2-trifluoroethyl) ether (BTFE)[87], are usually considered as ideal candidates as a diluent due to their low viscosity, sufficient electrochemical stability, appropriate miscibility, and poor solvating capability. The addition of diluents separates the bulk and interfacial responsibilities of an electrolyte and assigns these roles to varying phases that are microscopically separated[66]. Because the diluent does not coordinate with the cations, the immediate local environment of cations and anions still maintains the solvation structure of HCE (Figure 5d), which is often responsible for the interphasial chemistries at electrode surfaces[66]. The simultaneous stabilization of lithium metal, and high capacity and high voltage cathodes is attributed to the highly fluorinated CEI and SEI as decomposition products of the anions. Meanwhile, the average bulk properties are improved by the preferred ion transport, viscosity, or wettability of the diluent.

4.3 Solid State Electrolyte

As mentioned in the previous section, the Li metal anode by definition has the highest theoretical energy density among any other anode materials of LIBs. However, the electronic and ionic conductive Li dendrite can penetrate the porous separator and make direct contact with the cathode, leading to the internal short circuit of the batteries. Moreover, uneven precipitation of active materials will lead to their losing contact with the anode, forming electrochemically “dead” Li and causing permanent capacity loss. Even though novel electrolyte additives, such as FEC, can provide an improved cycling performance, potential risks of thermal runaway still exist, hindering the practical applications of lithium metal anodes. To seek a permanent solution to the challenge, one straightforward approach is substituting the conventional separator and liquid electrolyte design with high-mechanical-strength and dense solid-state electrolytes (SSEs). SSEs mainly fall into three categories: inorganic solid electrolytes, polymer solid electrolytes, and composite SSEs.

Among recent advances in inorganic solid electrolytes, predominant types of materials include garnet-type SSE ($Li_7La_3Zr_2O_{12}$, LLZO)[88], $Li_7P_3S_{11}$ (LPS)[89], $Li_{14}A_{l0.4}Ti_{1.6}(PO_4)_3$ (LATP)[90], and their analogues. Inorganic SSEs exhibit satisfactory ionic conductivity, mechanical properties, and excellent electrochemical stability against Li metal. Notably, some of them have ionic conductivity comparable to or even surpassing that of liquid electrolytes ($1 \sim 10\ mS\cdot cm^{-1}$)[7]. However, a trade-off exists where high elastic modulus typically leads to poor surface adhesion and high interfacial resistance. To circumvent the challenge, remedy strategies have been explored including engineering an interfacial layer between lithium metal and SSEs[91], and surface treatment of SSEs to reduce interfacial resistance and increase lithiophilicity[92]. Polymer solid electrolytes based on lithium salts in polymer matrices exhibit favorable interfacial contact with Li metal and low cost[93]. However, the performance of polymer solid electrolytes is limited by low ionic conductivity[7], low lithium ion transference number[44], and unsatisfactory elastic modulus[94] compared with inorganic crystalline electrolytes. Continuous efforts have been made to further improve their mechanical/electrochemical stability and ionic conductivity, e.g., introducing mechanical reinforcement blocks[95], incorporating single-ion conductors that replace lithium salts[96], and double layer designs that balance the performance metrics[97, 98].

Recently, several composite SSEs designs have been proposed that combine ceramic nanoparticles/nanowires with the polymer[99-102]. Zhao et al.[103] developed an anion-immobilized solid-state composite electrolyte (PLL) synthesized by a Garnet-type Al-doped $Li_{6.75}La_3Zr_{1.75}Ta_{0.25}O_{12}$, polyethylene oxide (PEO), and LiTFSI, where TFSI anions were effectively immobilized due to their interactions with ceramic particles and polymer matrix, as shown in Figure 6. As a result, a high transference number, low polarization, and uniform ion distribution were achieved. However, even with improved Li dendrite suppression, interfacial adhesion, and transference number, the reported ionic conductivity of composite SSEs is still one to two orders of magnitude lower than that of

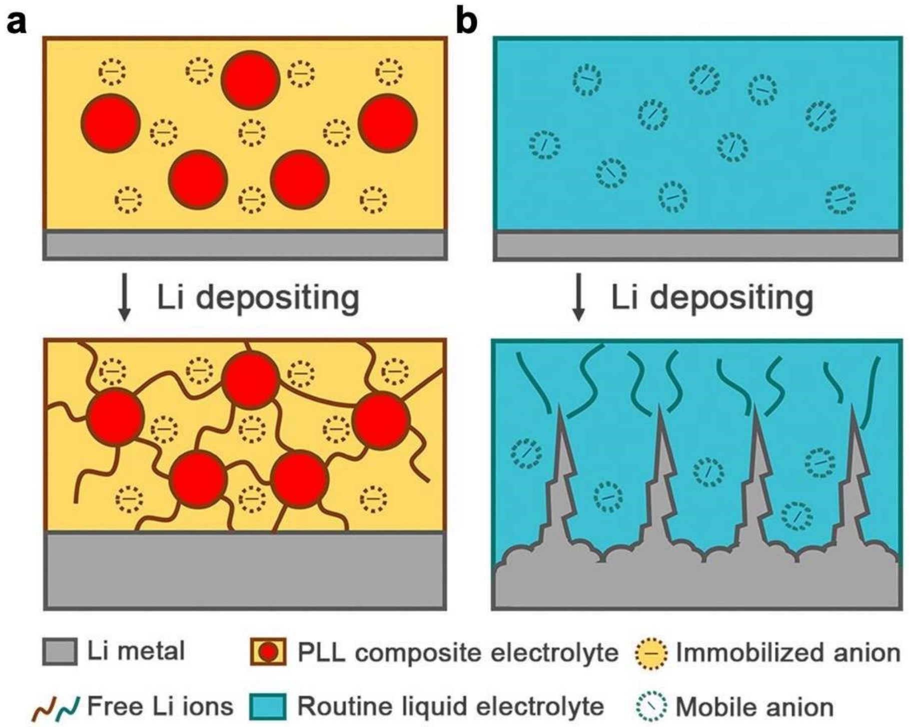

Figure 6 (a) Schematic of the electrochemical deposition behavior of the Li metal anode with the PLL solid electrolyte with immobilized anions and (b) the routine liquid electrolyte with mobile anions. Reproduced with permission from ref [103]. Copyright 2017 National Academy of Sciences. (color on line)

liquids, which is insufficient to fulfill the demand for batteries with high energy density and high charging rate.

One of the practical approaches to address above mentioned challenges is the use of quasi-solid-state electrolytes (QSSEs), i.e., adding a minimum amount of liquid electrolytes (organic solvents or ionic liquid) into solid electrolytes (polymer or inorganic material)[104, 105]. Recently, anionic metal-organic frameworks (MOFs) with superior ionic conductivity and Li^+ transference numbers have opened a new avenue in the development of QSSEs. To immobilize anions on the backbone of these frameworks, one approach is to directly link negatively charged building blocks, whereby the lithium counterions are introduced as the only mobile species inside the material. For example, Xu et al.[105] reported a 3-fold interpenetrating anionic MOF (MOF-688) synthesized from Anderson type polyoxometalate (POM) $[N(C_4H_9)_4]_3[MnMo_6O_{18}\{(OCH_2)_3CNH_2\}_2]$(MnMo$_6$) and tetrakis(4-formylphenyl)methane (TFPM) building units through imine condensation, as shown in Figure 7a. With PC filling the pores, Li^+-exchanged MOF-688 exhibited a high ionic conductivity of $4.0 \times 10^{-4}\ S\cdot cm^{-1}$ and high Li^+ transference number of 0.87 at 298 K.

In this new class of promising prototype QSSEs, it is important to understand the transport and conduction mechanisms, especially given the characterization challenges associated with transport measurements[44, 106, 107]. Therefore, Hou and Xu et al.[108] further performed theoretical and experimental investigations on the topic, and proposed the first theoretical model that accurately described the ionic conduction mechanism of MOF-based QSSEs. Two 3-fold interpenetrating anionic MOFs, the original MOF-688 ($[(MnMo_6)_2(TFPM)]$imine) and a newly synthesized isoreticular structure, $[(AlMo_6)_2(TFPM)]$imine, were considered. Using a suite of modeling approaches to elucidate the ionic diffusion, the primary ionic conduction mechanism was identified as solvent assisted

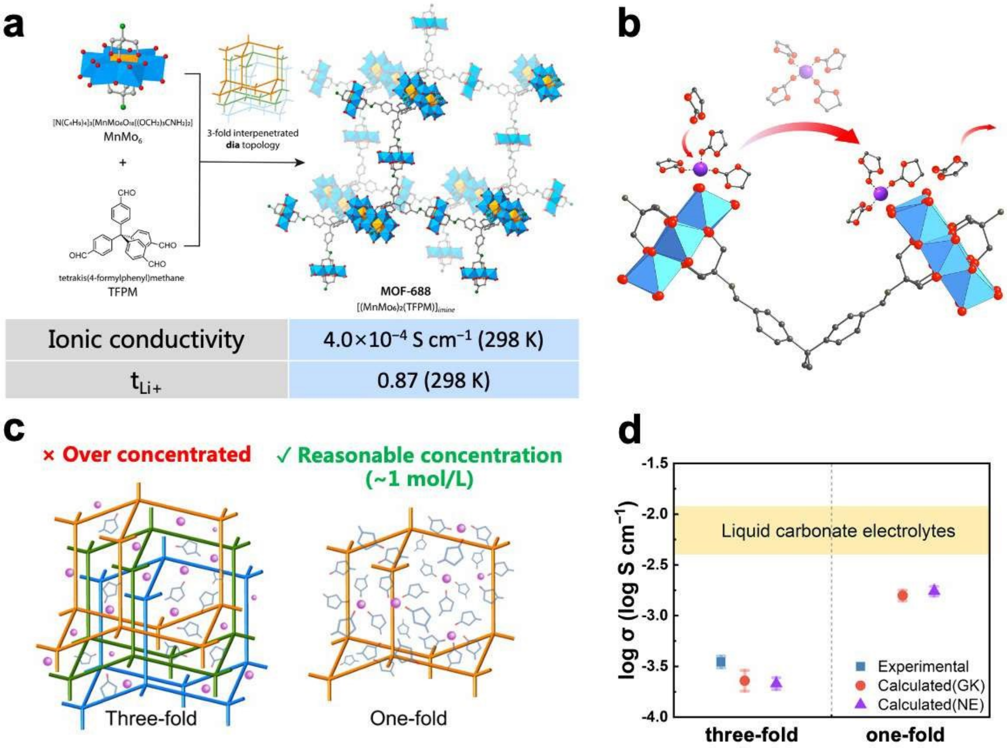

Figure 7 (a) Synthetic strategy, structure illustration and key performance of QSSE based on MOF-688. Reprinted with permission from ref [105]. Copyright 2019 American Chemical Society. (b) Scheme of solvent-assisted hopping. (c) Schemes of MOF-688 QSSEs with three-fold and proposed one-fold interpenetrating structures. (d) Ionic conductivity comparison plot of MOF-688 (three-fold) and MOF-688 (one-fold), and the conductivity range of liquid carbonate electrolytes (highlighted). Reprinted with permission from ref [108]. Copyright 2022 The Authors. (color on line)

hopping (> 77%), as illustrated in Figure 7b. Based on the prevalent mechanism of Li^+ motion, a hypothesized MOF design with a non-interpenetrating structure (Figure 7c) was proposed to achieve 6 ~ 8 times better performance (1.6 ~ 1.7 mS·cm^{-1}) than the current state-of-the-art (0.19 ~ 0.35 mS·cm^{-1}), approach ing the conductivity range of liquid electrolytes (Figure 7d). The mechanistic insights and design principles are deemed beneficial for future improvements of QSSEs within this category and beyond.

5 Conclusions and Outlooks

Traditional spectroscopic techniques have played an irreplaceable role in deciphering the coordination chemistry of electrolyte in the bulk phase. What is more, the application of surface-enhanced Raman spectroscopy (SERS)[109] has allowed the direct probing of the Li^+ solvation structure in the immediate vicinity (~ 20 nm) of the solid electrode-liquid interface. Recently, the utilization of tip-enhanced Raman spectroscopy (TERS)[110] has even pushed the limit of interfacial/interphasial characterization to the nanoscale chemical and topographical heterogeneity of the SEI. Thus, there remains vast opportunities in the development and application of novel experimental tools for extending our knowledge of the electrode-electrolyte interface. Meanwhile, atomistic modeling emerges as a powerful approach for evaluating and designing electrolytes for LIBs and beyond. Computational tools such as MD, quantum chemistry and kMC methods have been reported to model the solvation structure, transport properties, mechanical properties as well as the electrochemical reactivity/stability of electrolyte systems ranging from liquid electrolytes to (quasi-)solid-state electrolytes. Although a certain level of assumptions is (and must be) made, the obtained calculation results are in fair agreement with experiments in these reports. With the innovation of modeling methods and the booming of advanced computing power of CPUs and GPUs, atomistic modeling will be able to provide faster and more accurate predictions of electrolyte properties as well as mechanistic understandings of novel electrolyte systems that are challenging to obtain from experiments[111]. Therefore, theoretical simulations are expected to transform from an assistive tool to an indispensable part of the research and development of electrolytes.

As conventional electrolytes have been optimized for over two decades, linear modifications and adjustments are no longer effective to significantly improve the performance and the scope of application of electrolytes. Thus, screening candidate molecules/materials and their composites in a broader chemical space cannot be bypassed in pursuit of novel electrolytes for next-generation energy storage. From this perspective, we propose several theoretical approaches that are considered possible to cope with these challenges. First, a standardized and transplantable framework that can theoretically predict electrolyte properties is highly useful for exploring candidate electrolytes in a large scale. Notably, the development of high-throughput computation methods (e.g., automatic job submission) and deliberately designed simulation procedures (e.g., wisely choosing a realistic performance descriptor) are two crucial aspects of building an efficient and precise instance of such frameworks. Second, developing and applying high-accuracy first-principle methods will aid in the precise prediction of electrolyte reactions. The more accurate the thermodynamics/energetics are, the more confident we are in determining the reaction sequence and products of the reaction cascade. For example, the recent advances in meta-GGA methods have boosted the accuracy of reaction calculations to a higher level. Third, statistic learning methods can be employed to train atomistic force fields or build a direct predictive model of electrolyte properties[112]. In the future, multidisciplinary, collaborative, and persistent development efforts are required to achieve the ultimate smart design of novel electrolyte materials.

Acknowledgements

C.T. gratefully acknowledges financial support from the Australian Research Council through the Discovery Early Career Researcher Award (DE220101365).

References:

[1] Yang Y S. A review of electrochemical energy storage researches in the past 22 years[J]. J. Electrochem., 2020, 26 (4): 443-463.

[2] Hou T Z, Peng H J, Huang J Q, Zhang Q, Li B. The formation of strong-couple interactions between nitrogen-doped graphene and sulfur/lithium (poly)sulfides in lithium-sulfur batteries[J]. 2D Mater., 2015, 2(1): 014011.

[3] Lun Z, Ouyang B, Kwon D H, Ha Y, Foley E E, Huang T Y, Cai Z, Kim H, Balasubramanian M, Sun Y, Huang J, Tian Y, Kim H, McCloskey B D, Yang W, Clement R J, Ji H, Ceder G. Cation-disordered rocksalt-type high-entropy cathodes for Li-ion batteries[J]. Nat. Mater., 2021, 20(2): 214-221.

[4] Clément R J, Lun Z, Ceder G. Cation-disordered rocksalt transition metal oxides and oxyfluorides for high energy lithium-ion cathodes[J]. Energy Environ. Sci., 2020, 13(2): 345-373.

[5] Manthiram A, Fu Y, Chung S H, Zu C, Su Y S. Rechargeable lithium-sulfur batteries[J]. Chem. Rev., 2014, 114(23): 11751-11787.

[6] Chen X, Li X, Mei D, Feng J, Hu M Y, Hu J, Engelhard M, Zheng J, Xu W, Xiao J, Liu J, Zhang J G. Reduction mechanism of fluoroethylene carbonate for stable solid-electrolyte interphase film on silicon anode[J]. ChemSusChem, 2014, 7(2): 549-554.

[7] Lin D C, Liu Y Y, Cui Y. Reviving the lithium metal anode for high-energy batteries[J]. Nat. Nanotechnol., 2017, 12(3): 194-206.

[8] Xu K. Nonaqueous liquid electrolytes for lithium-based rechargeable batteries[J]. Chem. Rev., 2004, 104(10): 4303-4418.

[9] Cheng X B, Zhang R, Zhao C Z, Zhang Q. Toward safe lithium metal anode in rechargeable batteries: A review[J]. Chem. Rev., 2017, 117(15): 10403-10473.

[10] Schroder K, Alvarado J, Yersak T A, Li J, Dudney N, Webb L J, Meng Y S, Stevenson K J. The effect of fluoroethylene carbonate as an additive on the solid electrolyte interphase on silicon lithium-ion electrodes[J]. Chem. Mater., 2015, 27(16): 5531-5542.

[11] Cheng X B, Yan C, Chen X, Guan C, Huang J Q, Peng H J, Zhang R, Yang S T, Zhang Q. Implantable solid electrolyte interphase in lithium-metal batteries[J]. Chem, 2017, 2(2): 258-270.

[12] Hou T, Yang G, Rajput N N, Self J, Park S W, Nanda J, Persson K A. The influence of FEC on the solvation structure and reduction reaction of $LiPF_6$/EC electrolytes and its implication for solid electrolyte interphase formation[J]. Nano Energy, 2019, 64: 103881.

[13] Blau S M, Patel H D, Spotte-Smith E W C, Xie X, Dwaraknath S, Persson K A. A chemically consistent graph architecture for massive reaction networks applied to solid-electrolyte interphase formation[J]. Chem. Sci., 2021, 12 (13): 4931-4939.

[14] Shi S Q, Lu P, Liu Z Y, Qi Y, Hector L G, Li H, Harris S J. Direct calculation of Li-ion transport in the solid electrolyte interphase[J]. J. Am. Chem. Soc., 2012, 134(37): 15476-15487.

[15] Shi S, Qi Y, Li H, Hector L G. Defect thermodynamics and diffusion mechanisms in Li_2Co_3 and implications for the solid electrolyte interphase in Li-ion batteries[J]. J. Phys. Chem. C, 2013, 117(17): 8579-8593.

[16] Aurbach D, Zaban A, Schechter A, Ein-Eli Y, Zinigrad E, Markovsky B. The study of electrolyte solutions based on ethylene and diethyl carbonates for rechargeable Li batteries: I. Li metal anodes[J]. J. Electrochem. Soc., 1995, 142(9): 2873-2882.

[17] Xu K, Lam Y, Zhang S S, Jow T R, Curtis T B. Solvation sheath of Li^+ in nonaqueous electrolytes and its implication of graphite/electrolyte interface chemistry[J]. J. Phys. Chem. C, 2007, 111(20): 7411-7421.

[18] Wang L, Menakath A, Han F, Wang Y, Zavalij P Y, Gaskell K J, Borodin O, Iuga D, Brown S P, Wang C, Xu K, Eichhorn B W. Identifying the components of the solid-electrolyte interphase in Li-ion batteries[J]. Nat. Chem., 2019, 11(9): 789-796.

[19] Seo D M, Chalasani D, Parimalam B S, Kadam R, Nie M, Lucht B L. Reduction reactions of carbonate solvents for lithium ion batteries[J]. ECS Electrochem. Lett., 2014, 3(9): A91-A93.

[20] Philippe B, Dedryvère R, Gorgoi M, Rensmo H, Gonbeau D, Edström K. Role of the $LiPF_6$ salt for the long-term stability of silicon electrodes in Li-ion batteries — a photoelectron spectroscopy study[J]. Chem. Mater., 2013, 25 (3): 394-404.

[21] Yoon T, Milien M S, Parimalam B S, Lucht B L. Thermal decomposition of the solid electrolyte interphase (SEI) on silicon electrodes for lithium ion batteries [J]. Chem. Mater., 2017, 29(7): 3237-3245.

[22] Parimalam B S, MacIntosh A D, Kadam R, Lucht B L. Decomposition reactions of anode solid electrolyte interphase (SEI) components with $LiPF_6$[J]. J. Phys. Chem. C, 2017, 121(41): 22733-22738.

[23] Jurng S, Brown Z L, Kim J, Lucht B L. Effect of electrolyte on the nanostructure of the solid electrolyte interphase (SEI) and performance of lithium metal anodes[J]. Energy Environ. Sci., 2018, 11(9): 2600-2608.

[24] Etacheri V, Marom R, Elazari R, Salitra G, Aurbach D. Challenges in the development of advanced Li-ion batteries: a review[J]. Energy Environ. Sci., 2011, 4(9): 3243.

[25] Galushkin N E, Yazvinskaya N N, Galushkin D N. Mechanism of gases generation during lithium-ion batteries cycling[J]. J. Electrochem. Soc., 2019, 166(6): A897-A908.

[26] Hou T, Fong K D, Wang J, Persson K A. The solvation structure, transport properties and reduction behavior of carbonate-based electrolytes of lithium-ion batteries [J]. Chem. Sci., 2021, 12(44): 14740-14751.

[27] Liang C, Kwak K, Cho M. Revealing the solvation structure and dynamics of carbonate electrolytes in lithium-ion batteries by two-dimensional infrared spectrum modeling [J]. J. Phys. Chem. Lett., 2017, 8(23): 5779-5784.

[28] Seo D M, Reininger S, Kutcher M, Redmond K, Euler W B, Lucht B L. Role of mixed solvation and ion pairing in the solution structure of lithium ion battery electrolytes [J]. J. Phys. Chem. C, 2015, 119(25): 14038-14046.

[29] Pekarek R T, Affolter A, Baranowski L L, Coyle J, Hou T, Sivonxay E, Smith B A, McAuliffe R D, Persson K A, Key B, Apblett C, Veith G M, Neale N R. Intrinsic chemical reactivity of solid-electrolyte interphase components in silicon-lithium alloy anode batteries probed by FTIR spectroscopy[J]. J. Mater. Chem. A, 2020, 8(16): 7897-7906.

[30] Giorgini M G, Futamatagawa K, Torii H, Musso M, Cerini S. Solvation structure around the Li^+ ion in mixed cyclic/linear carbonate solutions unveiled by the Raman noncoincidence effect[J]. J. Phys. Chem. Lett., 2015, 6 (16): 3296-3302.

[31] Allen J L, Borodin O, Seo D M, Henderson W A. Combined quantum chemical/raman spectroscopic analyses of Li^+ cation solvation: cyclic carbonate solvents—ethylene carbonate and propylene carbonate[J]. J. Power Sources, 2014, 267: 821-830.

[32] Su C C, He M, Amine R, Rojas T, Cheng L, Ngo A T, Amine K. Solvating power series of electrolyte solvents for lithium batteries[J]. Energy Environ. Sci., 2019, 12(4): 1249-1254.

[33] Su C C, He M, Amine R, Chen Z, Amine K. The relationship between the relative solvating power of electrolytes and shuttling effect of lithium polysulfides in lithium-sulfur batteries[J]. Angew. Chem. Int. Ed., 2018, 57(37): 12033-12036.

[34] Borodin O, Olguin M, Ganesh P, Kent P R, Allen J L, Henderson W A. Competitive lithium solvation of linear and cyclic carbonates from quantum chemistry[J]. Phys. Chem. Chem. Phys., 2016, 18(1): 164-175.

[35] Zhang X, Kuroda D G. An Ab initio molecular dynamics study of the solvation structure and ultrafast dynamics of lithium salts in organic carbonates: a comparison between linear and cyclic carbonates[J]. J. Chem. Phys., 2019, 150 (18): 184501.

[36] Tang Z K, Tse J S, Liu L M. Unusual Li-ion transfer mechanism in liquid electrolytes: a first-principles study [J]. J. Phys. Chem. Lett., 2016, 7(22): 4795-4801.

[37] Skarmoutsos I, Ponnuchamy V, Vetere V, Mossa S. Li^+ solvation in pure, binary, and ternary mixtures of organic carbonate electrolytes[J]. J. Phys. Chem. C, 2015, 119(9): 4502-4515.

[38] Vatamanu J, Borodin O, Smith G D. Molecular dynamics simulation studies of the structure of a mixed carbonate/$LiPF_6$ electrolyte near graphite surface as a function of electrode potential[J]. J. Phys. Chem. C, 2011, 116(1): 1114-1121.

[39] Boyer M J, Vilciauskas L, Hwang G S. Structure and Li^+ ion transport in a mixed carbonate/$LiPF_6$ electrolyte near graphite electrode surfaces: a molecular dynamics study [J]. Phys. Chem. Chem. Phys., 2016, 18(40): 27868-27876.

[40] Shim Y. Computer simulation study of the solvation of lithium ions in ternary mixed carbonate electrolytes: free energetics, dynamics, and ion transport[J]. Phys. Chem. Chem. Phys., 2018, 20(45): 28649-28657.

[41] Yao N, Chen X, Shen X, Zhang R, Fu Z H, Ma X X, Zhang X Q, Li B Q, Zhang Q. An atomic insight into the chemical origin and variation of the dielectric constant in liquid electrolytes[J]. Angew. Chem. Int. Ed., 2021, 60 (39): 21473-21478.

[42] Tenney C M, Cygan R T. Analysis of molecular clusters in simulations of lithium-ion battery electrolytes[J]. J. Phys. Chem. C, 2013, 117(47): 24673-24684.

[43] Liu H, Maginn E. A molecular dynamics investigation of the structural and dynamic properties of the ionic liquid 1-N-butyl-3-methylimidazolium bis(trifluoromethanesulfonyl)imide[J]. J. Chem. Phys., 2011, 135(12): 124507.

[44] Fong K D, Self J, Diederichsen K M, Wood B M, McCloskey B D, Persson K A. Ion transport and the true transference number in nonaqueous polyelectrolyte solutions for lithium ion batteries[J]. ACS Cent. Sci., 2019, 5 (7): 1250-1260.

[45] Fong K D, Bergstrom H K, McCloskey B D, Mandadapu K K. Transport phenomena in electrolyte solutions: nonequilibrium thermodynamics and statistical mechanics[J]. AICHE J., 2020, 66(12): e17091.

[46] Fong K D, Self J, McCloskey B D, Persson K A. Onsager transport coefficients and transference numbers in polyelectrolyte solutions and polymerized ionic liquids [J]. Macromolecules, 2020, 53(21): 9503-9512.

[47] Ringsby A J, Fong K D, Self J, Bergstrom H K, McCloskey B D, Persson K A. Transport phenomena in low temperature lithium-ion battery electrolytes[J]. J. Electrochem. Soc., 2021, 168(8): 080501.

[48] Fong K D, Self J, McCloskey B D, Persson K A. Ion correlations and their impact on transport in polymer-based electrolytes[J]. Macromolecules, 2021, 54(6): 2575-2591.

[49] Spotte-Smith E W C, Kam R L, Barter D, Xie X, Hou T, Dwaraknath S, Blau S M, Persson K A. Toward a mechanistic model of solid-electrolyte interphase formation and evolution in lithium-ion batteries[J]. ACS Energy Lett., 2022, 7(4): 1446-1453.

[50] Graetz J, Ahn C C, Yazami R, Fultz B. Highly reversible lithium storage in nanostructured silicon[J]. Electrochem. Solid-State Lett., 2003, 6(9): A194-A197.

[51] Schweidler S, de Biasi L, Schiele A, Hartmann P, Brezesinski T, Janek J. Volume changes of graphite anodes revisited: a combined operando X-ray diffraction and *in situ* pressure analysis study[J]. J. Phys. Chem. C, 2018, 122(16): 8829-8835.

[52] Xu K. Electrolytes and interphases in Li-ion batteries and beyond[J]. J. Phys. Chem. C, 2014, 114(23): 11503-11618.

[53] Chen X, Shen X, Li B, Peng H J, Cheng X B, Li B Q, Zhang X Q, Huang J Q, Zhang Q. Ion-solvent complexes promote gas evolution from electrolytes on a sodium metal anode[J]. Angew. Chem. Int. Ed., 2018, 57(3): 734-737.

[54] Zhang X Q, Chen X, Cheng X B, Li B Q, Shen X, Yan C, Huang J Q, Zhang Q. Highly stable lithium metal batteries enabled by regulating the solvation of lithium ions in nonaqueous electrolytes[J]. Angew. Chem. Int. Ed., 2018, 57(19): 5301-5305.

[55] Nguyen C C, Lucht B L. Comparative study of fluoroethylene carbonate and vinylene carbonate for silicon anodes in lithium ion batteries[J]. J. Electrochem. Soc., 2014, 161(12): A1933-A1938.

[56] Philippe B, Dedryvere R, Gorgoi M, Rensmo H, Gonbeau D, Edstrom K. Improved performances of nanosilicon electrodes using the salt LiFSI: A photoelectron spec-

troscopy study[J]. J. Am. Chem. Soc., 2013, 135(26): 9829-9842.

[57] Xu W, Wang J, Ding F, Chen X, Nasybulin E, Zhang Y, Zhang J G. Lithium metal anodes for rechargeable batteries[J]. Energy Environ. Sci., 2014, 7(2): 513-537.

[58] Sun Y M, Liu N A, Cui Y. Promises and challenges of nanomaterials for lithium-based rechargeable batteries[J]. Nat. Energy, 2016, 1(7): 16071.

[59] Ding F, Xu W, Graff G L, Zhang J, Sushko M L, Chen X, Shao Y, Engelhard M H, Nie Z, Xiao J, Liu X, Sushko P V, Liu J, Zhang J G. Dendrite-free lithium deposition via self-healing electrostatic shield mechanism[J]. J. Am. Chem. Soc., 2013, 135(11): 4450-4456.

[60] Zhang X Q, Cheng X B, Chen X, Yan C, Zhang Q. Fluoroethylene carbonate additives to render uniform Li deposits in lithium metal batteries[J]. Adv. Funct. Mater., 2017, 27(10): 1605989.

[61] Qian J, Henderson W A, Xu W, Bhattacharya P, Engelhard M, Borodin O, Zhang J G. High rate and stable cycling of lithium metal anode[J]. Nat. Commun., 2015, 6: 6362.

[62] Xia Y, Zheng J M, Wang C M, Gu M. Designing principle for Ni-rich cathode materials with high energy density for practical applications[J]. Nano Energy, 2018, 49: 434-452.

[63] Hou T Z, Xu W T, Chen X, Peng H J, Huang J Q, Zhang Q. Lithium bond chemistry in lithium-sulfur batteries[J]. Angew. Chem. Int. Ed., 2017, 56(28): 8178-8182.

[64] Hou T Z, Chen X, Peng H J, Huang J Q, Li B Q, Zhang Q, Li B. Design principles for heteroatom-doped nanocarbon to achieve strong anchoring of polysulfides for lithium-sulfur batteries[J]. Small, 2016, 12(24): 3283-3291.

[65] Rajput N N, Murugesan V, Shin Y, Han K S, Lau K C, Chen J, Liu J, Curtiss L A, Mueller K T, Persson K A. Elucidating the solvation structure and dynamics of lithium polysulfides resulting from competitive salt and solvent interactions[J]. Chem. Mater., 2017, 29(8): 3375-3379.

[66] Borodin O, Self J, Persson K A, Wang C, Xu K. Uncharted waters: super-concentrated electrolytes[J]. Joule, 2020, 4 (1): 69-100.

[67] Shkrob I A, Wishart J F, Abraham D P. What makes fluoroethylene carbonate different? [J]. J. Phys. Chem. C, 2015, 119(27): 14954-14964.

[68] Xu C, Lindgren F, Philippe B, Gorgoi M, Björefors F, Edström K, Gustafsson T. Improved performance of the silicon anode for Li-ion batteries: understanding the surface modification mechanism of fluoroethylene carbonate as an effective electrolyte additive[J]. Chem. Mater., 2015, 27(7): 2591-2599.

[69] Sina M, Alvarado J, Shobukawa H, Alexander C, Manichev V, Feldman L, Gustafsson T, Stevenson K J, Meng Y /S. Direct visualization of the solid electrolyte interphase and its effects on silicon electrochemical performance[J]. Adv. Mater. Interfaces, 2016, 3(20): 1600438.

[70] Shi F, Ross P N, Somorjai G A, Komvopoulos K. The chemistry of electrolyte reduction on silicon electrodes revealed by *in situ* ATR-FTIR spectroscopy[J]. J. Phys. Chem. C, 2017, 121(27): 14476-14483.

[71] Schroder K W, Celio H, Webb L J, Stevenson K J. Examining solid electrolyte interphase formation on crystalline silicon electrodes: influence of electrochemical preparation and ambient exposure conditions[J]. J. Phys. Chem. C, 2012, 116(37): 19737-19747.

[72] Breitung B, Baumann P, Sommer H, Janek J, Brezesinski T. *In situ* and operando atomic force microscopy of high-capacity nano-silicon based electrodes for lithium-ion batteries[J]. Nanoscale, 2016, 8(29): 14048-14056.

[73] Yoon I, Abraham D P, Lucht B L, Bower A F, Guduru P R. *In situ* measurement of solid electrolyte interphase evolution on silicon anodes using atomic force microscopy[J]. Adv. Energy Mater., 2016, 6(12): 1600099.

[74] Young B T, Heskett D R, Nguyen C C, Nie M, Woicik J C, Lucht B L. Hard X-ray photoelectron spectroscopy (HAXPES) investigation of the silicon solid electrolyte interphase (SEI) in lithium-ion batteries[J]. ACS Appl. Mater. Interfaces, 2015, 7(36): 20004-20011.

[75] Jin Y, Kneusels N H, Magusin P, Kim G, Castillo-Martinez E, Marbella L E, Kerber R N, Howe D J, Paul S, Liu T, Grey C P. Identifying the structural basis for the increased stability of the solid electrolyte interphase formed on silicon with the additive fluoroethylene carbonate[J]. J. Am. Chem. Soc., 2017, 139(42): 14992-15004.

[76] Schiele A, Breitung B, Hatsukade T, Berkes B B, Hartmann P, Janek J, Brezesinski T. The critical role of fluoroethylene carbonate in the gassing of silicon anodes for lithium-ion batteries[J]. ACS Energy Lett., 2017, 2(10): 2228-2233.

[77] Zhang Y Y, Su M, Yu X F, Zhou Y F, Wang J G, Cao R G, Xu W, Wang C M, Baer D R, Borodin O, Xu K, Wang Y T, Wang X L, Xu Z J, Wang F Y, Zhu Z H. Investigation of ion-solvent interactions in nonaqueous electrolytes using *in situ* liquid SIMS[J]. Anal. Chem., 2018, 90(5): 3341-3348.

[78] Stetson C, Yoon T, Coyle J, Nemeth W, Young M, Norman A, Pylypenko S, Ban C, Jiang C S, Al-Jassim M, Burrell A. Three-dimensional electronic resistivity map-

ping of solid electrolyte interphase on Si anode materials [J]. Nano Energy, 2019, 55: 477-485.

[79] Shobukawa H, Alvarado J, Yang Y, Meng Y S. Electrochemical performance and interfacial investigation on Si composite anode for lithium ion batteries in full cell[J]. J. Power Sources, 2017, 359: 173-181.

[80] He J, Wang H P, Zhou Q, Qi S H, Wu M G, Li F, Hu W, Ma J M. Unveiling the role of Li^+ solvation structures with commercial carbonates in the formation of solid electrolyte interphase for lithium metal batteries[J]. Small Methods, 2021, 5(8): e2100441.

[81] Yamada Y, Yamada A. Review—superconcentrated electrolytes for lithium batteries[J]. J. Electrochem. Soc., 2015, 162(14): A2406-A2423.

[82] Yamada Y, Wang J, Ko S, Watanabe E, Yamada A. Advances and issues in developing salt-concentrated battery electrolytes[J]. Nat. Energy, 2019, 4(4): 269-280.

[83] Suo L M, Borodin O, Gao T, Olguin M, Ho J, Fan X L, Luo C, Wang C S, Xu K. “Water-in-salt” electrolyte enables high-voltage aqueous lithium-ion chemistries [J]. Science, 2015, 350(6263): 938-943.

[84] Borodin O, Suo L M, Gobet M, Ren X M, Wang F, Faraone A, Peng J, Olguin M, Schroeder M, Ding M S, Gobrogge E, Cresce A V, Munoz S, Dura J A, Greenbaum S, Wang C S, Xu K. Liquid structure with nano-heterogeneity promotes cationic transport in concentrated electrolytes [J]. ACS Nano, 2017, 11(10): 10462-10471.

[85] Self J, Fong K D, Persson K A. Transport in superconcentrated $LiPF_6$ and $LiBF_4$/propylene carbonate electrolytes [J]. ACS Energy Lett., 2019, 4(12): 2843-2849.

[86] Cao X, Jia H, Xu W, Zhang J G. Review—localized high-concentration electrolytes for lithium batteries[J]. J. Electrochem. Soc., 2021, 168(1): 010522.

[87] Chen S, Zheng J, Mei D, Han K S, Engelhard M H, Zhao W, Xu W, Liu J, Zhang J G. High-voltage lithium-metal batteries enabled by localized high-concentration electrolytes[J]. Adv. Mater., 2018, 30(21): 1706102.

[88] Murugan R, Thangadurai V, Weppner W. Fast lithium ion conduction in garnet-type $Li_7La_3Zr_2O_{12}$ [J]. Angew. Chem. Int. Ed., 2007, 46(41): 7778-7781.

[89] Wenzel S, Weber D A, Leichtweiss T, Busche M R, Sann J, Janek J. Interphase formation and degradation of charge transfer kinetics between a lithium metal anode and highly crystalline $Li_7P_3S_{11}$ solid electrolyte[J]. Solid State Ion., 2016, 286: 24-33.

[90] Aono H, Sugimoto E, Sadaoka Y, Imanaka N, Adachi G Y. Ionic conductivity of the lithium titanium phosphate? ($Li_{1+x}MXTi_{2-x}(PO_4)_3$, M = Al, Sc, Y, and La) systems[J]. J. Electrochem. Soc., 2019, 136(2): 590-591.

[91] Luo W, Gong Y H, Zhu Y Z, Li Y J, Yao Y G, Zhang Y, Fu K, Pastel G, Lin C F, Mo Y F, Wachsman E D, Hu L B. Reducing interfacial resistance between garnet-structured solid-state electrolyte and Li-metal anode by a germanium layer[J]. Adv. Mater., 2017, 29(22): 1606042.

[92] Huo H Y, Chen Y, Zhao N, Lin X T, Luo J, Yang X F, Liu Y L, Guo X X, Sun X L. *In-situ* formed Li_2Co_3-free garnet/Li interface by rapid acid treatment for dendrite-free solid-state batteries[J]. Nano Energy, 2019, 61: 119-125.

[93] Qin K, Holguin K, Mohammadiroudbari M, Huang J, Kim E Y S, Hall R, Luo C. Strategies in structure and electrolyte design for high-performance lithium metal batteries[J]. Adv. Funct. Mater., 2021, 31(15): 2009694.

[94] Brissot C, Rosso M, Chazalviel J N, Lascaud S. Dendritic growth mechanisms in lithium/polymer cells[J]. J. Power Sources, 1999, 81-82: 925-929.

[95] Singh M, Odusanya O, Wilmes G M, Eitouni H B, Gomez E D, Patel A J, Chen V L, Park M J, Fragouli P, Iatrou H, Hadjichristidis N, Cookson D, Balsara N P. Effect of molecular weight on the mechanical and electrical properties of block copolymer electrolytes[J]. Macromolecules, 2007, 40(13): 4578-4585.

[96] Bouchet R, Maria S, Meziane R, Aboulaich A, Lienafa L, Bonnet J P, Phan T N, Bertin D, Gigmes D, Devaux D, Denoyel R, Armand M. Single-ion BAB triblock copolymers as highly efficient electrolytes for lithium-metal batteries[J]. Nat. Mater., 2013, 12(5): 452-457.

[97] Zhou W D, Wang Z X, Pu Y, Li Y T, Xin S, Li X F, Chen J F, Goodenough J B. Double-layer polymer electrolyte for high-voltage all-solid-state rechargeable batteries[J]. Adv. Mater., 2019, 31(4): 1805574.

[98] Stone G M, Mullin S A, Teran A A, Hallinan D T, Minor A M, Hexemer A, Balsara N P. Resolution of the modulus versus adhesion dilemma in solid polymer electrolytes for rechargeable lithium metal batteries[J]. J. Electrochem. Soc., 2012, 159(3): A222-A227.

[99] Duan H, Fan M, Chen W P, Li J Y, Wang P F, Wang W P, Shi J L, Yin Y X, Wan L J, Guo Y G. Extended electrochemical window of solid electrolytes via heterogeneous multilayered structure for high-voltage lithium metal batteries[J]. Adv. Mater., 2019, 31(12): 1807789.

[100] Cheng Q, Li A J, Li N, Li S, Zangiabadi A, Li T D, Huang W L, Li A C, Jin T W, Song Q Q, Xu W H, Ni N, Zhai H W, Dontigny M, Zaghib K, Chuan X Y, Su D, Yan K, Yang Y. Stabilizing solid electrolyte-anode interface in Li-metal batteries by boron nitride-based nanocomposite coating[J]. Joule, 2019, 3(6): 1510-1522.

[101] Liu W, Liu N, Sun J, Hsu P C, Li Y, Lee H W, Cui Y. Ionic conductivity enhancement of polymer electrolytes

with ceramic nanowire fillers[J]. Nano Letters, 2015, 15 (4): 2740-2745.

[102] Zhou W D, Wang S F, Li Y T, Xin S, Manthiram A, Goodenough J B. Plating a dendrite-free lithium anode with a polymer/ceramic/polymer sandwich electrolyte [J]. J. Am. Chem. Soc., 2016, 138(30): 9385-9388.

[103] Zhao C Z, Zhang X Q, Cheng X B, Zhang R, Xu R, Chen P Y, Peng H J, Huang J Q, Zhang Q. An anion-immoblized composite electrolyte for dendrite-free lithium metal anodes[J]. Proc. Natl. Acad. Sci. U.S.A, 2017, 114(42): 11069-11074.

[104] Judez X, Martinez-Ibañez M, Santiago A, Armand M, Zhang H, Li C M. Quasi-solid-state electrolytes for lithium sulfur batteries: advances and perspectives[J]. J. Power Sources, 2019, 438: 226985.

[105] Xu W, Pei X, Diercks C S, Lyu H, Ji Z, Yaghi O M. A metal-organic framework of organic vertices and polyoxometalate linkers as a solid-state electrolyte[J]. J. Am. Chem. Soc., 2019, 141(44): 17522-17526.

[106] Cronau M, Szabo M, König C, Wassermann T B, Roling B. How to measure a reliable ionic conductivity? The stack pressure dilemma of microcrystalline sulfide-based solid electrolytes[J]. ACS Energy Lett., 2021, 6(9): 3072-3077.

[107] Winand J M, Depireux J. Measurement of ionic conductivity in solid electrolytes[J]. Europhys. Lett., 1989, 8(5): 447-452.

[108] Hou T, Xu W, Pei X, Jiang L, Yaghi O M, Persson K A. Ionic conduction mechanism and design of metal-organic framework based quasi-solid-state electrolytes[J]. J. Am. Chem. Soc., 2022, 144(30): 13446-13450.

[109] Yang G, Ivanov I N, Ruther R E, Sacci R L, Subjakova V, Hallinan D T, Nanda J. Electrolyte solvation structure at solid-liquid interface probed by nanogap surface-enhanced Raman spectroscopy[J]. ACS Nano, 2018, 12(10): 10159-10170.

[110] Nanda J, Yang G, Hou T, Voylov D N, Li X, Ruther R E, Naguib M, Persson K, Veith G M, Sokolov A P. Unraveling the nanoscale heterogeneity of solid electrolyte interphase using tip-enhanced Raman spectroscopy [J]. Joule, 2019, 3(8): 2001-2019.

[111] Chen X, Zhang Q. Atomic insights into the fundamental interactions in lithium battery electrolytes[J]. Acc. Chem. Res., 2020, 53(9): 1992-2002.

[112] Yao N, Chen X, Fu Z H, Zhang Q. Applying classical, *ab initio,* and machine-learning molecular dynamics simulations to the liquid electrolyte for rechargeable batteries[J]. Chem. Rev., 2022, 122(12): 10970-11021.

当前和下一代锂离子电池电解液的原子尺度微观认识和研究进展

侯廷政[1,2*],陈　翔[4],蒋　璐[1],唐　城[3,4*]

(1. 加利福尼亚大学伯克利分校材料科学与工程系,伯克利 加利福尼亚 94706,美国; 2. 清华大学深圳国际研究生院,
深圳 广东 518055, 中华人民共和国; 3. 阿德莱德大学化学工程与先进材料学院,
阿德莱德 南澳大利亚 5005, 澳大利亚; 4. 清华大学化学工程系,北京 100084,中华人民共和国)

摘要: 电解液及构筑电极电解液界面对于开发和应用高比容量储能系统至关重要。具体来说,电解液的机械(抗压性、粘度)、热(热导率和热容)、化学(溶解性、活度、反应性)、输运和电化学(界面及界面层)等性质,与其所组成的储能器件的性能直接相关。目前,大量的实验研究通过调控电解液的物理和/或化学组成来改善电解液性能,以满足新型电极材料的工作运行。与此同时,理论模拟方法近年来得到了迅速发展,使人们可以从原子尺度来理解电解液在控制离子输运和构筑功能化界面的作用。站在理论模拟研究的前沿上, 人们可以利用其所揭示的机理性认识对新型电解液开展理性设计。本文首先总结了传统电解液的组成、溶剂化结构和输运性质以及电极电解液界面层的形成机理,进一步讨论了利用新型电解液设计稳定电极电解液界面层的方法,包括使用电解液添加剂、高浓电解液和固态电解质,并着重讨论了对这些新型电解液体系进行原子尺度模拟的最新进展,为了解和认识电解液提供更为基本的理解,并为未来电解液的设计提供系统的指导。最后,作者对新型电解液的理论筛选进行了展望。

关键词: 锂离子电池;电解液;原子模拟;固体电解质界面层;固态电解质